



HAL
open science

Quadsight® Vision System in Adverse Weather Maximizing the benefits of visible and thermal cameras

Pierre Duthon, Nadav Edelstein, Efi Zelentzer, Frederic Bernardin

► **To cite this version:**

Pierre Duthon, Nadav Edelstein, Efi Zelentzer, Frederic Bernardin. Quadsight® Vision System in Adverse Weather Maximizing the benefits of visible and thermal cameras. 2022 12th International Conference on Pattern Recognition Systems (ICPRS), Jun 2022, Saint-Etienne, France. pp.1-6, 10.1109/ICPRS54038.2022.9854076 . hal-03762797

HAL Id: hal-03762797

<https://hal.science/hal-03762797>

Submitted on 29 Aug 2022

HAL is a multi-disciplinary open access archive for the deposit and dissemination of scientific research documents, whether they are published or not. The documents may come from teaching and research institutions in France or abroad, or from public or private research centers.

L'archive ouverte pluridisciplinaire **HAL**, est destinée au dépôt et à la diffusion de documents scientifiques de niveau recherche, publiés ou non, émanant des établissements d'enseignement et de recherche français ou étrangers, des laboratoires publics ou privés.

Quadsight® Vision System in Adverse Weather

Maximizing the benefits of visible and thermal cameras

Pierre Duthon
STI research team
Cerema
Clermont-Ferrand, France
adweather@cerema.fr
0000-0002-6705-1131

Nadav Edelstein
Field Application Engineer
Foresight Automotive
Nes Ziona, Israel
nadave@foresightauto.com

Efi Zelentzer
Project Management
Foresight Automotive
Nes Ziona, Israel
efiz@foresightauto.com

Frédéric Bernardin
STI research team
Cerema
Clermont-Ferrand, France
adweather@cerema.fr
0000-0002-1248-153X

Abstract— Autonomous vehicles are currently one of the most popular research topics in computer vision. United Nations Economic Commission for Europe recently proposed a regulation for SAE level 3 automated driving systems. The current Operational Design Domains (ODD) are highway, slow speed (i.e. traffic jam), and clear weather conditions. Research is steadily creeping towards a focus on harsh weather conditions. There are now two major issues to investigate: (1) knowing how to characterize ODD and (2) extending ODD to include ‘new’ conditions. This investigation is being carried out within the framework of the AWARD project at Cerema’s PAVIN platform. Foresight Automotive’s QuadSight® vision system was tested under a range of artificially reproduced weather conditions. The novelty of this work is to present results of a 3D object detection ODD characterization: (a) on a commercially ready system, (b) using visible and thermal wavelengths, and (c) in controlled fog and rain conditions. The use of dual visible and long-wave infrared thermal sensors in stereo is essential to the all-weather detection of pedestrians and vehicles. The thermal sensor is essential in challenging conditions such as nighttime or adverse weather conditions. Rain and low lighting conditions pose no problem for the QuadSight system. The system also performs well in foggy conditions, with the only exception of compromised performance in very dense fog.

Keywords— *thermal camera, visible light camera, stereo camera, 3D object detection, adverse weather, fog, rain*

I. INTRODUCTION

Vision sensors are now commonly used to perceive the environment, detect surrounding objects, and make driving decisions. United Nations Economic Commission for Europe (UNECE) [1] recently proposed a regulation for SAE level 3 automated driving systems [2]. The regulation defines the Operational Design Domains (ODD) that correspond to the use cases which are validated, and in which the vehicle is able to drive in autonomous mode. The current research is focused on unusual or difficult environmental conditions. These include harsh weather conditions, dense traffic scenarios, urban areas, poorly surfaced or damaged roads, abnormal behaviors of other road users, and edge-cases. Two major issues remain concerning the use of vehicle perception systems (sensors and associated algorithms): (i) knowing how to characterize and verify the ODD, and (ii) to extend it to include new conditions.

The work presented here was carried out using Foresight’s QuadSight vision system at the PAVIN (Auvergne Platform for Smart Vehicles - Fog-Rain regional platform), allowing for the simulation of various scenarios and weather conditions. This work is part of the AWARD (All Weather Autonomous Real logistics operations and Demonstrations) project [3]. This project is a 3-year innovation action performed by a consortium of 29 partners. AWARD’s objective is to bring disruptive changes in the logistic industry, by scaling the autonomous vehicles and the logistics operation & fleet management systems for heavy-duty vehicles, targeting compliance with ISO 26262 and taking into consideration Safety of The Intended Functionality recommendations. The vehicles’ Autonomous Driving System (ADS) will be based on multiple sensor modalities and an embedded, teleoperation system to address 24/7 availability. The ADS will subsequently be integrated into multiple vehicle types commonly found in low-speed areas. Finally, these vehicles will be deployed, integrated and operated in a variety of real-life use-cases to validate their value in such applications, and to identify limitations and functional levels. These challenges will be tackled by extending the autonomous vehicles’ performance under the harsh weather conditions (i.e. rain, fog, snow) that are limiting the current ODD. These are to be developed alongside an adapted regulatory framework for autonomous logistics operations in warehouses, airports, and ports.

According to the latest published literature, most of the 3D object detection studies address only favorable climatic conditions. This is the case of most of the datasets in the field [4], [5], [6], [7]. Some recent datasets deal with adverse weather conditions, but only address visible light cameras and contain only few images [8] [9]. Other datasets that include many images exist for traffic surveillance applications [10] [11], fog removal [12] [13] [14] [15] [16] [17] or weather classification [10] [11]. These do not concern 3D object detection for automotive purposes and they do not contain thermal images. Concerning automotive sensors for autonomous driving, some recently published studies propose algorithms to deal with fog conditions by incorporating data fusion from LiDAR and stereoscopic visible light cameras [18] [19] [20]. Other studies analyze the impact of fog, rain and snow on LiDARs [21] [22] [23]. These studies do not use thermal cameras, such as the QuadSight vision system, for detection. Some other studies use data fusion with the use of thermal cameras [24] [25] but they don’t address adverse weather conditions.

The novelty of this work is to present results of 3D object detection: (a) on a commercialized system, (b) using visible light and thermal wavelengths, (c) in controlled fog and rain conditions. This document is the result of a collaboration between a commercial entity (Foresight and its proprietary QuadSight vision system and associated algorithm solution) and an academic institution (Cerema, ITS research team), allowing for the characterization of the ODD, and the scientific analysis on a commercialized system. The following section presents the characteristics of the QuadSight system. Section III describes the methodology used. Section IV shows the results of the investigation. Section V offers a conclusion to the study.

II. THE QUADSIGHT VISION SYSTEM

Foresight's proprietary technology (Fig. 1) is based on the utilization of 3D video analysis and advanced image processing algorithms to achieving unprecedented and accurate obstacle detection in adverse environmental conditions. This technology is revolutionizing automotive safety by providing automotive-grade, cost-effective solutions individually tailored to suit a wide range of markets. Foresight positions itself as a strategic fit for applications including passenger vehicles, heavy machinery (construction, mining and agriculture), robotics, and defense. This technology can be customized to address the numerous challenges facing Advanced Driver Assistance Systems and autonomous vehicles. The QuadSight system consists of 2 pairs of stereoscopic vision channels: a visible light stereo channel in conjunction with a thermal stereo channel, providing depth perception to obtain a clear 3D view of the environment.



Fig. 1 QuadSight vision system by Foresight (<https://www.foresightauto.com/solutions/quadsight/>)

Stereoscopic vision technology uses two synchronized cameras to generate a depth map, allowing for the detection of an object, either classified or non-classified, and its accurate size, location, and distance. Monocular vision object detection technologies are usually based upon inferencing and rely on Deep Neural Networks (DNN) object recognition. Using DNN for object recognition will always encounter corner cases where there is an unknown object to the trained network. Foresight's stereoscopic technology provides a hybrid detection solution for both classified and non-classified objects.

III. TESTING METHOD

TABLE I. SUMMARY OF THE METHODOLOGY

| | Scenario 1 | Scenario 2 |
|------------------------------------|----------------------------|------------------------------|
| Aim | Raw data analysis | Detection algorithm analysis |
| Metric | Contrast | Precision and recall |
| Illumination | Day / Night | Day / Night |
| Weather | 1 clear + 3 rains + 3 fogs | 1 clear + 3 rains + 3 fogs |
| Target distance | 17, 22 and 27m | 10, 17 and 25m |
| Targets | Reference targets | Car and pedestrian |
| Total number of experiments | 42 | 84 |

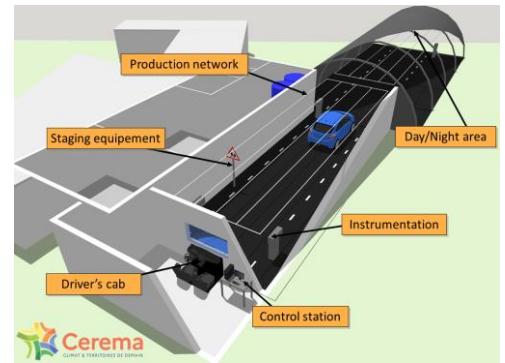


Fig. 2 Cerema's PAVIN Fog and Rain platform

Cerema's PAVIN platform is a 30m long and 5m wide enclosure in which numerous test scenarios may be performed. Lighting conditions simulating day or night are made possible thanks to a removable black cover over the clear roof covering the far section of the testing complex (Fig. 2). Fog and rain of varying intensities may be produced on demand. Fog density may be replicated in the Meteorological Optical Range (MOR) range of 10m to 1000m. The droplet size distribution is representative of continental or maritime fogs. Rain conditions may be produced with rainfall rate ranging from 10 to 180mm/h. Finally, various scene elements can be located in the test chamber to recreate calibrated test scenarios (i.e. reference targets) or real-world scenarios (i.e. road markings, traffic signs, vehicles, and pedestrians).

The MOR [26] is defined as the maximum distance (in meters) at which a calibrated object is visibly distinct from its background. The lower the MOR, the denser the fog. Fog with a MOR of 10m is considered extremely dense and is occasionally encountered on roads. For the sake of comparison, fog formed with a small average droplet size (0.8 microns) was produced (similar to a continental fog).

Rain intensity [26] is characterized by the rainfall rate in mm/h, corresponding to the height of water in mm that falls on a surface area of 1m² over a 60-minute period. The greater the rainfall rate, the heavier the rain. A rainfall rate of 120mm/h represents violent storm peaks in Europe.



Fig. 3. Presentation of the different targets used during the test. From left to right : Scenario 1 with reference targets, for visible light (a) and thermal cameras (b), Scenario 2 with pedestrian and car, for visible light (c) and thermal cameras (d.)

Two types of complementary tests, referred to as scenarios 1 and 2, are detailed below:

- Scenario 1 consists of characterizing the raw output of the sensor. This is made possible by performing a contrast measurement on calibrated targets. The targets are composed of: (i) Three Zenith Polymer targets with uniform reflectivity of 5%, 50% and 90%. The targets may be seen at the bottom of Fig.3(a). They allow for the measurement of the contrast on the visible light channel of the QuadSight system. (ii) Four black body thermal targets with surface temperatures of 30°C, 40°C, 50°C and 60°C. These targets can be found at the top of Fig. 3(b). They allow for the measurement of the contrast on the thermal channel of the QuadSight system.
- Scenario 2 characterizes the quality of object detection of the QuadSight system in poor weather conditions. The QuadSight system software allows 3D detection of various objects, in this case, vehicles and pedestrians. As seen in Fig. 3(c), a human pedestrian producing a true-to-life thermal signature, and an electric Renault Kangoo vehicle have been used as test subjects.

In both scenarios, various target-sensor distances, weather and illumination conditions combinations are tested. The targets are moved to differing distances as shown in Fig. 4. For each of these target-sensor distances, different operating conditions are addressed. These include day/night, fog of varying densities (MOR = 10m, 20m and 50m), and rain of varying intensities (rainfall rate = 11mm/h, 70mm/h and 120mm/h).

In daylight conditions, only the ambient light is present. In nightlight conditions, the headlights of the vehicle on which the QuadSight system is placed are turned on. In total, for scenario 1, we have 42 experiments (2 illumination conditions [day + night] x 7 weather conditions [1 clear + 3 rains + 3 fogs] x 3 target-sensor distances [17, 22 and 27m]). For scenario 2, we have 84 experiments (2 targets [car + pedestrian] x 2 illumination conditions [day + night] x 7 weather conditions [1 clear + 3 rains + 3 fogs] x 3 target-sensor distances [10, 17 and 25m]). Table I gives a synthesis of the methodology.

For the analysis of scenario 1, a contrast measurement of the images was used to verify the impact of the various weather conditions on the sensors. A region of interest on each of the calibrated targets was defined. The brightest and darkest targets were employed to measure the contrast. For the visible light sensor images, the Zenith polymer reference targets with reflectivity of 5% and 90% are used. For the images of the thermal sensor, the black body targets at 30°C and 60°C are used.

We define I_{wh} and I_{bk} as the average intensity values in the regions of interest of the reference targets. I_{wh} (white) is the average value of the Zenith polymer 90% target (resp. the black body target at 60°C) for the visible light (resp. thermal) sensor. I_{bk} (black) is the average value of the Zenith polymer 5% target (resp. the black body target at 30°C) for the visible light (resp. thermal) sensor. From this, we define the contrast C_i for experiment i (a particular target-sensor distance, weather, and lighting condition) taken from the set of experiments, using the following formula:

$$C_i = \frac{I_{wh} - I_{bk}}{I_{wh}}$$

As the contrast C_i uses a different scale for the visible light and thermal sensors, due to the dynamic range of the two sensors being different), we define a relative contrast K_i as follows:

$$K_i = \frac{C_i}{C_d} \times 100$$

where C_d is the contrast for experiment d at the same target-sensor distance and the same illumination condition as for experiment i , albeit measured in clear weather conditions. In this manner, the relative contrast K_i is always 100% for normal conditions (without fog or rain), and it degrades with the introduction of increasing rain and fog. This relative contrast will make it easier to compare the impact of weather conditions between both sensors. In some special cases, the relative contrast K_i can exceed 100%. This is the case if the contrast (C_i) in adverse weather conditions is better than the reference contrast (C_d) in clear weather. This can happen occasionally, in light fog or light rain conditions, if the illumination conditions and sensor settings are better than for reference conditions.

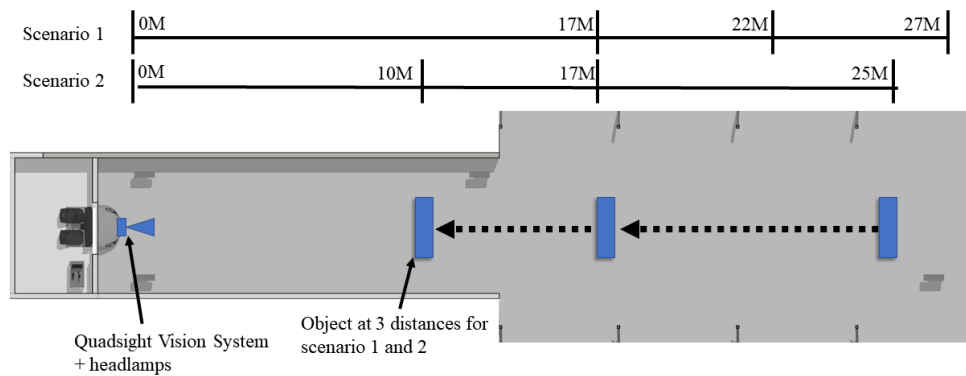


Fig. 4. Plan of the experiment. During the experiment, the object was : reference targets during scenario 1, pedestrian or car during scenario 2. For each target and at each position, different environmental conditions were applied (day, night, clear, fog, rain).

For the analysis of scenario 2, the measures of precision and recall were used. First, the position of the pedestrian and the vehicle over the entire dataset was manually annotated. The 3D object detection algorithm was then applied to the images. To determine whether a detection is valid, the Intersection of Union (IOU) metric was utilized. IOUs of 0.5 for pedestrian and 0.7 for a vehicle were used in this research. These are common state of the art values. A detection may thus be either a true positive (TP) or a false positive (FP). If a labeled object is not detected, it is considered to be a false negative (FN). The precision (P) and the recall (R) are defined as:

$$P = \frac{TP}{TP + FP} \quad R = \frac{TP}{TP + FN}$$

Precision and recall for each of the 84 experiments of scenario 2 were calculated. The method used for scenarios 1 and 2 is now clearly established. The following section presents the results obtained.

IV. RESULTS

Table II presents the results obtained for contrast measurements recorded for scenario 1. The results illustrate the advantages of using thermal cameras, as the contrast results are higher compared to visible light cameras. Concerning thermal cameras, the relative contrasts remain largely unchanged in rain or fog conditions, during day and nighttime, except for an MOR of 10m. These low values correspond to fog conditions such that the image appears almost entirely uniform, the objects being completely obscured by the fog. That reduction in relative contrast, as the MOR dropped to 10m, is common across the board. As the relative contrast approaches zero, it becomes increasingly difficult to detect an object.

For visible light cameras, fog had a greater impact than rain on visibility, in both day & night conditions. The relative contrasts remain largely unchanged in rain conditions. In fog conditions, however, the relative contrasts reduce significantly as the MOR falls below 50m. During daytime, fog with an MOR of greater than 20m resulted in relative contrast values above 60% in the visible light channel. This can be explained by a difference in illumination in the test tunnel (refer to Figure 5b below), as a result of removing the cover over the greenhouse. It had a negative impact on the visibility of targets due to the blinding effect

TABLE II. SCENARIO 1 : CONTRAST RESULTS (IN %)

| Target distance → | | Visible camera | | | Thermal camera | | | |
|-------------------|-------|----------------|-----|-----|----------------|-----|-----|-----|
| | | 17m | 22m | 27m | 17m | 22m | 27m | |
| Day | Clear | 100 | 100 | 100 | 100 | 100 | 100 | |
| | Fog | 10m | 23 | 22 | 3 | 39 | 11 | 24 |
| | | 20m | 51 | 58 | 34 | 128 | 133 | 134 |
| | | 50m | 61 | 63 | 60 | 102 | 105 | 98 |
| | Rain | 11 mm/h | 124 | 106 | 92 | NaN | NaN | NaN |
| | | 70 mm/h | 79 | 72 | 46 | NaN | NaN | NaN |
| | | 120 mm/h | 107 | 112 | 113 | NaN | NaN | NaN |
| Night | Clear | 100 | 100 | 100 | 100 | 100 | 100 | |
| | Fog | 10m | 0 | 1 | 2 | 24 | 14 | 44 |
| | | 20m | 7 | 5 | 5 | 106 | 77 | 81 |
| | | 50m | 43 | 26 | 17 | 90 | 76 | 69 |
| | Rain | 11 mm/h | 97 | 95 | 89 | 123 | 109 | 93 |
| | | 70 mm/h | 73 | 63 | 40 | 119 | 101 | 102 |
| | | 120 mm/h | 85 | 82 | 68 | 106 | 80 | 82 |

*NaN values are due to wrong exposure setting. The invalidity of these ones was noted during data processing, whereas the sensors were not available any more at Cerema. It was therefore not possible to repeat these tests. However, the values under night conditions are similar for the thermal camera.

TABLE III. SCENARIO 2 : DETECTION RESULTS (PRECISION / RECALL)

| Target dist. → | | Pedestrian - IOU 0.5 | | | | | | Car - IOU 0.7 | | | | | |
|----------------|--------------|----------------------|---------|---------|---------|---------|---------|---------------|---------|---------|---------|---------|---------|
| | | VIS | | | IR | | | VIS | | | IR | | |
| | | 10m | 17m | 25m | 10m | 17m | 25m | 10m | 17m | 25m | 10m | 17m | 25m |
| Day | Clear | 100/100 | 100/100 | 100/100 | 100/100 | 100/100 | 100/100 | 100/100 | 100/100 | 100/100 | 100/100 | 100/100 | 100/100 |
| | Fog 10m | 100/100 | NaN | NaN | 100/100 | 100/100 | 100/100 | 100/100 | NaN | NaN | 97/100 | NaN | NaN |
| | Fog 20m | 96/100 | 99/100 | 99/100 | 100/100 | 100/100 | 100/100 | 100/100 | 100/100 | NaN | 100/100 | 100/100 | 100/100 |
| | Fog 50m | 100/100 | 100/100 | 100/100 | 100/100 | 100/100 | 100/100 | 100/100 | 100/100 | 100/100 | 100/100 | 100/100 | 100/100 |
| | Rain 11mm/h | 100/100 | 100/100 | 100/100 | 100/100 | 95/100 | 96/100 | 100/100 | 100/100 | 100/100 | 100/100 | 100/100 | 100/100 |
| | Rain 72mm/h | 100/100 | 98/100 | 99/69 | 100/100 | 100/100 | 100/100 | 100/99 | 100/100 | 100/100 | 99/100 | 98/100 | 100/100 |
| | Rain 120mm/h | 100/100 | 100/100 | 100/100 | 100/100 | 100/100 | 100/100 | 100/100 | 100/100 | 100/100 | 100/100 | 100/100 | 100/100 |
| Night | Clear | 100/100 | 100/100 | 100/100 | 100/100 | 100/100 | 100/100 | 100/100 | 100/100 | 100/100 | 100/100 | 100/100 | 100/100 |
| | Fog 10m | NaN | NaN | NaN | 98/100 | 100/100 | NaN | NaN | NaN | NaN | 97/100 | NaN | NaN |
| | Fog 20m | 100/92 | NaN | NaN | 98/100 | 98/100 | 98/100 | 100/100 | NaN | NaN | 98/100 | 96/100 | 78/93 |
| | Fog 50m | 100/100 | 100/99 | 100/56 | 100/100 | 98/100 | 100/100 | 100/100 | 100/100 | 97/100 | 100/100 | 100/100 | 100/100 |
| | Rain 11mm/h | 100/100 | 100/100 | 99/100 | 100/100 | 100/100 | 95/100 | 100/100 | 100/100 | 100/100 | 100/100 | 100/100 | 100/100 |
| | Rain 72mm/h | 100/100 | 100/100 | 100/97 | 100/100 | 100/100 | 81/57 | 100/100 | 98/100 | 98/99 | 100/100 | 96/100 | 100/100 |
| | Rain 120mm/h | 100/100 | 100/100 | 94/74 | 100/100 | 100/100 | 93/100 | 100/100 | 100/100 | 100/100 | 100/100 | 100/100 | 100/100 |

*NaN values - There was no visible detection of the objects at the listed ground truth distances.



Fig. 5. Different images to better understand the discussion. a. & b. Problem of exposure setup with thermal camera for day and rain conditions (a. wrong exposure, b. correct exposure). c. & d. Example of the pedestrian who is totally invisible on (c.) the visible light camera, while he is perfectly visible on (d.) the thermal camera. Both images (c. and d.) are taken at the same time and under the same conditions.

on the visible light camera sensor. In fog conditions there is a decrease in relative contrast proportional to the increase in both the target-sensor distance and the fog density. These findings are supported by the published literature [10].

The results of precision and recall scores are recorded in Table III. The results confirmed the expected system performance for both visible light and thermal channels based on past experimental data. The visible light cameras are highly dependent on the environmental lighting conditions and subsequently, show reduced performance at low lighting (night) levels. This is not the case for thermal cameras, however, as they are dependent entirely on object heat and emissivity. On this basis, the results of different lighting conditions do not show any change in performance.

The rain at all levels had minimal effect on the performance of both visible light and thermal channels.

The results show improved detection of pedestrian target compared to the electric car target at fog levels 10 and 20m. This can be explained by the difference in heat emissivity of pedestrian and car. As opposed to combustion engine vehicles which expel a large amount of heat, an electric vehicle is more similar in temperature to the surrounding environment. The improved detections of both pedestrian and car by the thermal channel compared to the visible light channel at fog 10 and 20m is explained by the reliance on object emissivity as opposed to lighting conditions. All fog scenes tests were performed immediately following the rain scenarios, while all objects were still wet, reducing contrast between the object and the surrounding environment. Sometimes the results drop slightly, but this can be explained by local variations in the test conditions, such as the exposure time setting or the position of the pedestrian.

V. CONCLUSION

The QuadSight system was tested in the Cerema's PAVIN platform under controlled harsh weather conditions: fog and rain at day and night lighting conditions. Scenario 1 verified the effectiveness of the visible light and thermal sensors by taking contrast measurements on calibrated targets, whilst scenario 2 dealt with object detections of both a pedestrian and a vehicle.

Despite technical complications during the testing period, Foresight's technology achieved quality results for both stereo vision light and thermal imaging. Combining the advantages of stereo systems using visible light and thermal cameras will increase road safety for all road users and will pave the way for better ADAS and autonomous vehicles. The thermal cameras enhance ADAS systems, allowing improved performance under many weather and lighting conditions. The concurrent use of these camera-based sensors provides a complete image of the surrounding environment, under challenging conditions, where other sensors' performance may be compromised.

Finally, a method to characterize an ODD has been presented here, under controlled weather conditions. This collaborative research effort, between a commercial body and an academic institution, allowed for an initial outline for this type of test. These tests in controlled adverse weather conditions will be completed by tests on tracks, within the framework of the AWARD project.

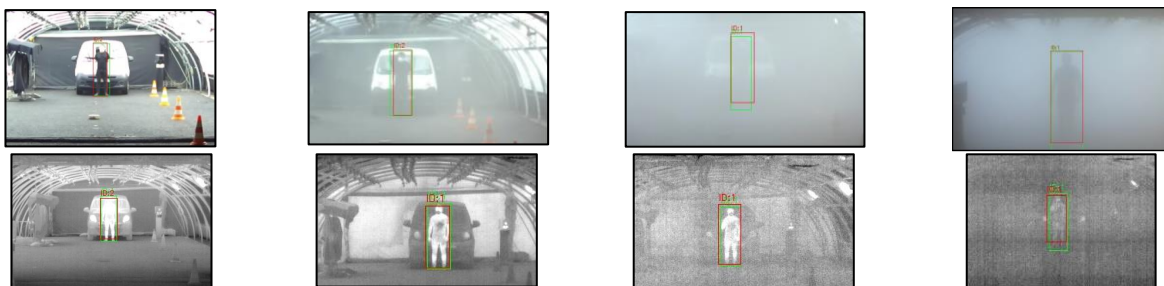


Fig. 6. Example of detection results, in fog conditions at the maximum distance of detection. From left to right : Clear, Fog 50m, Fog 20m, Fog 10m. Up: visible light camera, down: thermal camera.

ACKNOWLEDGMENT



This project has received funding from the European Union's Horizon 2020 research and innovation program under grant agreement No 101006817.

The content of this reflects only the author's view. Neither the European Commission nor CINEA is responsible for any use that may be made of the information it contains.

REFERENCES

- [1] U. N. E. C. for Europe (UNECE), «Proposal for a New UN Regulation on Uniform Provisions Concerning the Approval of Vehicles with Regards to Automated Lane Keeping System,» 2020.
- [2] S. A. E. International, *J3016 - Taxonomy and Definitions for Terms Related to On-Road Motor Vehicle Automated Driving Systems*, 2014, p. 12.
- [3] *AWARD Project*, <https://award-h2020.eu>, 2021.
- [4] P. Sun, H. Kretzschmar, X. Dotiwalla, A. Chouard, V. Patnaik, P. Tsui, J. Guo, Y. Zhou, Y. Chai, B. Caine, W. Han et al., *Scalability in Perception for Autonomous Driving: Waymo Open Dataset*, 2020.
- [5] H. Caesar, V. Bankiti, A. H. Lang, S. Vora, V. E. Liong, Q. Xu, A. Krishnan, Y. Pan, G. Baldan et O. Beijbom, *nuScenes: A multimodal dataset for autonomous driving*, 2020.
- [6] A. Geiger, P. Lenz et R. Urtasun, «Are we ready for autonomous driving? the kitti vision benchmark suite,» chez *2012 IEEE conference on computer vision and pattern recognition*, 2012.
- [7] F. Yu, W. Xian, Y. Chen, F. Liu, M. Liao, V. Madhavan et T. Darrell, «Bdd100k: A diverse driving video database with scalable annotation tooling,» *arXiv preprint arXiv:1805.04687*, vol. 2, p. 6, 2018.
- [8] K. Dahmane, P. Duthon, F. Bernardin, M. Colomb, N. E. B. Amara et F. Chausse, «The Cerema pedestrian database : A specific database in adverse weather conditions to evaluate computer vision pedestrian detectors,» 2016.
- [9] C. Sakaridis, D. Dai et L. Van Gool, «Semantic foggy scene understanding with synthetic data,» *International Journal of Computer Vision*, vol. 126, p. 973–992, 2018.
- [10] K. Dahmane, P. Duthon, F. Bernardin, M. Colomb, F. Chausse et C. Blanc, «WeatherEye-Proposal of an Algorithm Able to Classify Weather Conditions from Traffic Camera Images,» *Atmosphere*, vol. 12, 2021.
- [11] K. Dahmane, P. Duthon, F. Bernardin et M. Colomb, «Weather Classification with traffic surveillance cameras,» 2018.
- [12] C. Ancuti, C. O. Ancuti et R. Timofte, «Ntire 2018 challenge on image dehazing: Methods and results,» chez *Proceedings of the IEEE Conference on Computer Vision and Pattern Recognition Workshops*, 2018.
- [13] Y. Zhang, Y. Tian, Y. Kong, B. Zhong et Y. Fu, «Residual dense network for image super-resolution,» chez *Proceedings of the IEEE conference on computer vision and pattern recognition*, 2018.
- [14] S. Ki, H. Sim, J.-S. Choi, S. Kim et M. Kim, «Fully end-to-end learning based conditional boundary equilibrium gan with receptive field sizes enlarged for single ultra-high resolution image dehazing,» chez *Proceedings of the IEEE Conference on Computer Vision and Pattern Recognition Workshops*, 2018.
- [15] Y. Lei, T. Emaru, A. A. Ravankar, Y. Kobayashi et S. Wang, «Semantic Image Segmentation on Snow Driving Scenarios,» *2020 IEEE International Conference on Mechatronics and Automation (ICMA)*, pp. 1094-1100, 2020.
- [16] H. Sim, S. Ki, J.-S. Choi, S. Seo, S. Kim et M. Kim, «High-resolution image dehazing with respect to training losses and receptive field sizes,» chez *IEEE Conference on Computer Vision and Pattern Recognition*, 2018.
- [17] O. Kupyn, V. Budzan, M. Mykhailych, D. Mishkin et J. Matas, «Deblurgan: Blind motion deblurring using conditional adversarial networks,» chez *IEEE conference on computer vision and pattern recognition*, 2018.
- [18] N. A. M. Mai, P. Duthon, L. Khoudour, A. Crouzil et S. A. Velastin, «3D Object Detection with SLS-Fusion Network in Foggy Weather Conditions,» *Sensors*, vol. 21, 2021.
- [19] M. Bijelic, F. Mannan, T. Gruber, W. Ritter, K. Dietmayer et F. Heide, «Seeing Through Fog Without Seeing Fog: Deep Sensor Fusion in the Absence of Labeled Training Data,» *CoRR*, vol. abs/1902.0, 2019.
- [20] A. Pfeuffer et K. Dietmayer, «Robust semantic segmentation in adverse weather conditions by means of sensor data fusion,» chez *2019 22th International Conference on Information Fusion (FUSION)*, 2019.
- [21] Y. Li, P. Duthon, M. Colomb et J. Ibanez-Guzman, «What happens for a ToF LiDAR in fog? (accepted, under review),» *Transactions on Intelligent Transportation Systems*, 2020.
- [22] R. Heinzler, F. Piewak, P. Schindler et W. Stork, «Cnn-based lidar point cloud de-noising in adverse weather,» *IEEE Robotics and Automation Letters*, vol. 5, p. 2514–2521, 2020.
- [23] M. Kuttila, P. Pyykönen, W. Ritter, O. Sawade et B. Schäufele, «Automotive LIDAR sensor development scenarios for harsh weather conditions,» chez *2016 IEEE 19th ITSC*, 2016.
- [24] M.-g. Cho, «A Study on the Obstacle Recognition for Autonomous Driving RC Car Using LiDAR and Thermal Infrared Camera,» chez *2019 Eleventh International Conference on Ubiquitous and Future Networks (ICUFN)*, 2019.
- [25] V. John et S. Mita, «Deep Feature-Level Sensor Fusion Using Skip Connections for Real-Time Object Detection in Autonomous Driving,» *Electronics*, vol. 10, 2021.
- [26] W. M. Organization, *Guide to Meteorological Instruments and Methods of Observation (2014 edition updated in 2017; WMO-No. 8)*, World Meteorological Organization, 2014, p. 1163.